UDK 001.89:[616.98:578.834
546.27:519.876.5
COBISS.SR-ID 57391369

APPLICATION OF AN EFFICIENT ALGORITHM FOR OPTIMIZATION MIXTURE COMPOSITION OF BORONIZING PROCESS DURING THE COVID-19 PANDEMIC

Emina Požega[1]
Slavica Miletić[2]

[1,2] Mining and metallurgy Institute Bor, Zeleni bulevar 35, Bor, Serbia,
[1]emina.pozega@irmbor.co.rs
[2]slavica.miletic@irmbor.co.rs

ABSTRACT

Appearance of the covid-19 virus caused a social and economic disorder, a change in the world and people's lives. In order to reduce energy consumption, production costs, obtain high material utilization, reduce the number of experiments in difficult working conditions during the pandemic, a program for boronizing process simulation was applied. The paper presents application of an efficient algorithm for optimization mixture composition of boronizing process during the covid-19 pandemic.
The practical application of the tested composition of activators in the boride-based boron mixture on iron powder castings was achieved through obtaining materials with a quality boride layer and with characteristics that meet the conditions of application in modern industrial plants.
In order to apply the activator in the boron-based boronizing mixture as the most suitable ratios for obtaining quality boride layers, the obtained samples were characterized. A simplex plan with fifteen experimental points was used for the experiment, and a polynomial of the fourth degree was used for the mathematical model. The impact of the COVID-19 consequences on science and scientists, their works and researches is reduced this way.

KEYWORDS

COVID-19, analysis, evaluation, boronizing, boride layers

JEL: C3, O1

1. INTRODUCTION

Many authors have conducted research on the impact of the consequences caused by COVID-19 on economy, society, science, life and work of people and scientists (Segal & Gerstel, 2020; Paul & Chowdhury, 2020).

In this paper we will present the experience of our research group at the simultaneously sintering and boronizing process using an efficient algorithm for optimization mixture composition during the covid-19 pandemic.

Industrial applications of wear and corrosion resistant materials include: drive shafts, camshafts, pulleys, machine slide-ways, tanks, weapons and parts for agricultural machinery (İpek et al., 2000). Considerable economic loss occurs because of corrosion and wears in mechanical parts of machines and equipment during service. In order to reduce this loss, properties of the surface region of materials should be improved. One of the methods used to improve the surface quality is boriding (Meric et al., 2006; Selçuk et al., 2000; Stojanović & Stanisavljev, 2013; Stojanović et al., 2017; Özge et al., 2016; Makuch, 2020; Makuch et al., 2019). Boriding is a thermochemical surface hardening treatment in which boron atoms are diffused into the metal surface at elevated temperatures, usually between 1223 and 1373 K to form a hard layer of borides consisting of FeB and/or Fe2B, needle-like microstructure, of about 150 μm thick (Keddam, 2004; Hunger &Trute, 1994; Xu et al., 1997). The crystal structure is orthorhombic for FeB, while Fe2B has a body centered tetragonal structure (Ramirez et al., 2007). The diffusion of boron into the surface of selected samples creates a fully dense reaction zone of metal borides. This effectively generates superior surface properties of materials (Sen et al., 2005). A single-phase structure is desirable and Fe2B is preferred to FeB, since FeB is very hard and brittle. Furthermore, since FeB and Fe2B phases exhibit substantially different coefficients of thermal expansions, crack formation is often observed at the interface between FeB and Fe2B. These cracks often lead to flaking of the coated layer when mechanical load is applied. By controlling the boron activity of the boriding medium and chemical composition of the sample to be treated, it is possible to obtain a microstructure consisting of only Fe2B phase without the FeB phase (Sen et al., 2005; Campos et al., 2005). This process is similar in its physical and chemical characteristics to other surface hardening treatments, such as carburization and nitriding. The advantage of boriding over other types of surface hardening methods is that, the surface layer is very hard, friction coefficient is very low, no extra heat treatment is required after boriding and it has considerable resistance against some acid, base, metal solutions and high temperature oxidation. It has been successfully applied to all ferrous materials, nickel alloys, titanium alloys, sintered carbides (Sinha, 1991; Chatterjee, 1989) and sintered materials are significantly different from materials formed by conventional methods (casting, plastic deformation), both in structure and properties. One of the major differences in the structure is presence of porosity in these materials. Porosity, grain distortion, great length of grain boundaries are factors that significantly influence iron sintered material diffusion saturation processes. Boriding of a steel surface allows reducing essentially a velocity of corrosion, wear and shapes of fatigue cracks occurring in an outcome of its operation (Ozdemir, 2006). This process can be performed in solid, liquid or gaseous medium. The boriding in solid medium is technologically simpler and low cost, comparable to other boriding processes (Voroshnin et al., 1977; Požega, 2008; Allaoui et al., 2006; Celebi et al., 2005; Keddam & Chentouf, 2005; Dong et al., 2009). The boriding agent is in powder form. The boriding in solid medium can be carried out under inert atmosphere as well as in tightly closed boxes. Pack boriding method is a process similar to pack carburizing process (Genel et al., 2002; Erdemir & Bindal 1995). The knowledge of the boriding parameters, such as time, temperature, chemical composition and the activators percentage ratio, the composition of the basic mixture, are necessary for control and automation of the pack boriding process. Through the control of boriding process parameters, i.e. boriding powder composition, temperature, time, Fe2B phase can be consistently achieved during pack boriding (Jain & Sundararajan 2002).

Modelling and simulation, including computer simulation/calculation software (Berger et al., 2017) or program and mathematical representations of physics and chemistry of complex metallurgical systems, have been increasingly used to assist process development and design, process evaluation and optimization, production scheduling and planning, process control,

and business evaluation. Keddam et al. (Stojanović & Stanisavljev, 2013) developed the diffusion model based on Fick's laws. Their model has allowed simulation the growth kinetics of boride layers on the iron substrate. Kayacan, Şahin and Taştan proposed mathematical model which is based on the nonlinear Fourier law. Diffusion mechanism of the boriding process of AISI 1040 has been studied (Kayacan et al., 2010).

The growth kinetics of Fe2B boride layers generated at the surface of a gray cast iron via the powder-pack boriding was estimated by kinetic model (Keddam & Chegroune, 2010). By the use of the mass balance equation at the (Fe2B/sample) interface under certain assumptions and considering the effect of the boride incubation time, it was possible to estimate the corresponding parabolic growth constant for three process temperatures and four treatment times.

In this paper is presented an efficient algorithm for a software package of the fourth degree polynomial. The planned experiment represents a new approach to experimental research in which mathematical methods have an active role. Used algorithm for computer program, based on the regression equation, has enabled to obtain the volume change, porosity and depth coordinates and to draw a graph (simplex triangle) (Krasovsky & Filaretov, 1982).

The main interest has been focused on the choice of boriding mixture, activators and their relationship in order to obtain quality boride layers and to monitor certain events at boriding by algorithm for computer program.

2. MATERIAL AND METHODS

Experimental investigation executed in this study included: activators and mixtures composition for boriding choice, pressing pressure, temperature and boriding time. The characterization of iron powder was done as well as powders mixture homogenization, iron compacts formation, pressing samples characterization, boriding of pressed iron samples and their characterization, in order to determine influence of activators on constitution of diffusion layer compacts from iron powder at boriding process. Our own experience was used in selection of the boriding mixture, so the best results of the boride layer depth and quality were achieved using a mixture with boron carbide (B4C) and activators. NH4HF2, NH4Cl, and KBF4 were used as activators in the boriding process. The content of the basic components in the compound prepared for boriding was constant, but the activator's content was variable. The percentage share of the activator was different and it was in the range of 0 to 4 wt %. The regime of boriding was the same for all samples: the temperature was 1223 K and the process time was 4 hours. The samples obtained from iron powder NC 100.24 (Höganäs) by pressing under 400 MPa, had rectangular forms, with the cross-section dimensions of 31 mm × 12 mm.

In order to obtain reliable results the two samples were boroned under the same conditions.

The particles are sponge forms, which is characteristic of powders obtained by reduction. Iron powder characterization was carried out by determining the apparent density, outlet flow velocity, specific surface area, chemical and granulometric compositions. Samples were packed in a boriding box made of special steel. The box was then placed into an electrical resistance furnace for boriding. Samples were taken out from the box by removing the used boriding mixture when the box was gradually cooled to room temperature. In boriding treatment, as a result of boron diffusion into the surface, a boride layer in the upper surface of the boroned specimen was formed; just under this layer there was a diffusion zone and in the inner part was the base material. The boride layer, having toothed structure, was made up of iron-boride phases.

Samples dimensions before and after boriding are given in Table 1. The linear dimensions of samples, before and after boriding process on the basis of which the volume changes (in Table 2.) was determined, were measured with the precision of ± 0.01 mm. The porosity of samples was determined with the vacuum method. Samples porosity changes are given in Table 3. The boride layer depth was determined by a device for hardness measurement, with precision of ± 0.5 μm. For each sample the cross-section was measured eight times and the average values were calculated. The depth of boride formed on the samples surface is strongly dependent of activators. The obtained boride layer depth results are given in Table 4. The presence of borides formed on sample surfaces was identified by X - ray diffraction (XRD) measurements which were performed on the Siemens device "KRISTALLOFLEX 810". For recording is used Cu anti – cathode with filtered radiation, Ni filter, at voltage of 40 KV and current intensity of 20 mA. To compare changes in microstructure caused by boriding process, metallographic examination of boriding samples cross – section was carried out.

Table 1. *Dimensional changes before and after boriding*

number of samples	activators	h (mm)		b (mm)		l (mm)				
		h before	h after	b before	b after	l before	l after	Δ h[a] (%)	Δ b[a] (%)	Δ l[a] (%)
I	4%NH_4FHF	11.7	11.635	12.1	12.11	30.1	30.24	-0.556	0.083	0.465
		11.7	11.625	12.1	12.115	30.1	30.2	-0.641	0.124	0.332
II	4%NH_4Cl	11.6	11.61	12.1	12.16	30.1	30.22	0.086	0.496	0.399
		11.6	11.69	12.1	12.295	30.1	30.56	0.776	1.611	1.528
III	4%NH_4Cl	11.82	11.575	12.1	12.18	30.1	30.21	-2.073	0.661	0.365
		11.82	11.51	12.1	12.125	30.1	30.2	-2.623	0.207	0.332
IV	1%NH_4FHF 3%KBF_4	11.92	11.88	12.1	12.145	30.1	30.2	-0.336	0.372	0.332
		11.92	11.79	12.1	12.18	30.1	30.2	-1.091	0.661	0.332
V	2%NH_4FHF 2%KBF_4	11.22	11.21	12.1	12.13	30.1	30.19	-0.089	0.248	0.299
		11.27	11.27	12.1	12.125	30.1	30.17	0	0.207	0.232
VI	3%NH_4FHF 1%KBF_4	11.8	11.54	12.1	12.11	30.1	30.17	-2.204	0.083	0.232
		11.8	11.72	12.1	12.105	30.1	30.27	-0.678	0.041	0.565
VII	3%NH_4FHF 1%NH_4Cl	11.4	11.735	12.1	12.13	30.1	30.19	2.938	0.248	0.299
		11.57	11.54	12.1	12.135	30.1	30.21	-0.259	0.289	0.365
VIII	2%NH_4FHF 2%NH_4Cl	11.65	11.64	12.1	12.15	30.1	30.49	-0.086	0.413	1.296
		11.65	11.555	12.1	12.17	30.1	30.2	-0.815	0.578	0.332
IX	1%NH_4FHF 3%NH_4Cl	11.15	11.165	12.1	12.18	30.1	30.22	0.134	0.661	0.399
		11.22	11.315	12.1	12.2	30.1	30.25	0.847	0.826	0.498
X	3%NH_4Cl 1%KBF_4	12.05	12.135	12.1	12.635	30.1	30.37	0.705	4.421	0.897
		12	12.065	12.1	12.31	30.1	30.25	0.542	1.735	0.498
XI	2%NH_4Cl 2%KBF_4	11.4	11.34	12.1	12.125	30.1	30.25	-0.526	0.207	0.498
		11.4	11.675	12.1	12.14	30.1	30.25	2.412	0.330	0.498
XII	1%NH_4Cl 3%KBF_4	11.52	11.705	12.1	12.155	30.1	30.25	1.606	0.454	0.498
		11.82	11.535	12.1	12.145	30.1	30.2	-2.411	0.372	0.332
XIII	1%NH_4FHF 2%NH_4Cl 1%KBF_4	11.52	11.745	12.1	12.14	30.1	30.3	1.953	0.330	0.664
		11.85	11.59	12.1	12.135	30.1	30.19	-2.194	0.289	0.299
XIV	1%NH_4FHF 1%NH_4Cl 2%KBF_4	11.45	11.695	12.1	12.125	30.1	30.19	2.140	0.207	0.299
		11.4	11.615	12.1	12.11	30.1	30.18	1.886	0.083	0.266
XV	2%NH_4FHF 1%NH_4Cl 1%KBF_4	11.75	11.685	12.1	12.185	30.1	30.24	-0.553	0.702	0.465
		11.77	11.615	12.1	12.15	30.1	30.32	-1.317	0.413	0.731

[a] $\Delta h, \Delta b, \Delta l = \frac{h, b, l_{afterboridig} - h, b, l_{beforeboriding}}{h, b, l_{beforeboriding}} \cdot 100\%$

h, b, l_{after} – samples dimension (measure) after boriding [mm]

h, b, l_{before} – samples dimension (measure) before boriding (compact samples dimension) [mm]

Table 2. *Weight and volume changes before and after boriding*

number of samples	activators	m_1 (g) samples weight before boriding	m_2 (g) samples weight after boriding	Δm (g) weight of boroning layer	V_1 (cm^3) samples volume before boriding	V_2 (cm^3) samples volume after boriding	ΔV[b] (%) volume changes
I	4%NH_4FHF	24.91	25.53	0.62	4261.257	4260.811	-0.010
		24.98	25.59	0.61	4261.257	4253.274	-0.187
II	4%NH_4Cl	24.98	25.49	0.51	4224.836	4266.387	0.983
		24.94	25.72	0.78	4224.836	4392.344	3.965
III	4%NH_4Cl	25.01	25.42	0.41	4304.962	4259.112	-1.065
		24.98	25.36	0.38	4304.962	4214.674	-2.097
IV	1%NH_4FHF 3%KBF_4	25.02	25.49	0.47	4341.383	4357.335	0.367
		24.98	25.4	0.42	4341.383	4336.786	-0.106
V	2%NH_4FHF 2%KBF_4	25.07	25.48	0.41	4086.436	4105.155	0.458
		24.8	25.25	0.45	4104.647	4122.693	0.440
VI	3%NH_4FHF 1%KBF_4	24.99	25.53	0.54	4297.678	4216.239	-1.895
		25.01	25.46	0.45	4297.678	4294.423	-0.076
VII	3%NH_4FHF 1%NH_4Cl	24.99	25.74	0.75	4151.994	4297.412	3.502
		25.07	25.72	0.65	4213.91	4230.545	0.395
VIII	2%NH_4FHF 2%NH_4Cl	25.01	25.83	0.82	4243.047	4312.079	1.627
		25.01	25.68	0.67	4243.047	4246.855	0.090
IX	1%NH_4FHF 3%NH_4Cl	24.97	25.49	0.52	4060.942	4109.609	1.198
		24.84	25.49	0.65	4086.436	4175.801	2.187
X	3%NH_4Cl 1%KBF_4	24.92	25.72	0.8	4388.731	4656.502	6.101
		24.99	25.76	0.77	4370.52	4492.735	2.796
XI	2%NH_4Cl 2%KBF_4	24.96	25.56	0.6	4151.994	4159.299	0.176
		24.92	25.47	0.55	4151.994	4287.469	3.263
XII	1%NH_4Cl 3%KBF_4	24.29	24.96	0.67	4195.699	4303.797	2.576
		24.93	25.61	0.68	4304.962	4230.796	-1.723
XIII	1%NH_4FHF 2%NH_4Cl 1%KBF_4	25.03	25.51	0.48	4195.699	4320.304	2.970
		25.34	26.01	0.67	4315.889	4246.062	-1.618
XIV	1%NH_4FHF 1%NH_4Cl 2%KBF_4	24.81	25.5	0.69	4170.205	4280.999	2.657
		24.98	25.76	0.78	4151.994	4245.048	2.241
XV	2%NH_4FHF 1%NH_4Cl 1%KBF_4	24.91	25.62	0.71	4279.468	4305.623	0.611
		24.99	25.73	0.74	4286.752	4278.827	-0.185

[b] $\Delta V = ((V_2 - V_1)/V_1) \times 100\%$;

V_2 – samples volume after boriding

V_1 – volume of compacts

$\Delta m = ((m_2-m_1)/m_1) \times 100\%$;
m_2 – samples weight after boriding
m_1 – weight of compacts

Table 3. *Porosity of samples*

number of samples	activators	m_1 (g) samples weight before immersion	m_2 (g) samples weight after immersion	m_3 (g) oil mass	V (cm^3) samples volume	V (cm^3) pore volumes	Porosity[c] (%)
I	4%NH_4FHF	22.85	23.37	0.52	3.823	0.622	16.259
		22.94	23.47	0.53	3.817	0.633	16.600
II	4%NH_4Cl	21.82	22.33	0.51	3.638	0.610	16.760
		22.92	23.18	0.26	4.018	0.311	7.735
III	4% KBF_4	22.72	23.34	0.62	3.850	0.741	19.249
		22.53	23.17	0.64	3.820	0.765	20.029
IV	1%NH_4FHF 3%KBF_4	22.69	23.32	0.63	3.707	0.753	20.318
		22.31	22.9	0.59	3.589	0.705	19.652
V	2%NH_4FHF 2%KBF_4	22.59	22.81	0.22	3.614	0.263	7.277
		22.43	22.91	0.48	3.630	0.574	15.807
VI	3%NH_4FHF 1%KBF_4	22.99	23.6	0.61	4.056	0.729	17.978
		23.91	24.52	0.61	3.999	0.729	18.235
VII	3%NH_4FHF 1%NH_4Cl	23.03	23.16	0.13	3.920	0.155	3.964
		23.09	23.37	0.28	3.807	0.335	8.791
VIII	2%NH_4FHF 2%NH_4Cl	23.01	23.2	0.19	3.849	0.227	5.900
		22.99	23.08	0.09	3.792	0.107	2.837
IX	1%NH_4FHF 3%NH_4Cl	22.78	23	0.22	3.653	0.263	7.199
		22.86	22.98	0.12	3.716	0.143	3.861
X	3%NH_4Cl 1%KBF_4	23.22	23.52	0.3	3.987	0.359	8.994
		23.12	23.43	0.31	4.220	0.370	8.782
XI	2%NH_4Cl 2%KBF_4	22.92	23.08	0.16	3.707	0.191	5.160
		22.66	22.96	0.3	3.849	0.359	9.317
XII	1%NH_4Cl 3%KBF_4	22.35	22.63	0.28	4.057	0.335	8.249
		23.17	23.42	0.25	3.879	0.299	7.705
XIII	1%NH_4FHF 2%NH_4Cl 1%KBF_4	22.93	23.3	0.37	3.816	0.442	11.591
		23.04	23.19	0.15	3.666	0.179	4.891
XIV	1%NH_4FHF 1%NH_4Cl 2%KBF_4	22.97	23.16	0.19	3.935	0.227	5.7
		23.45	23.75	0.3	4.113	0.359	8.720
XV	2%NH_4FHF 1%NH_4Cl 1%KBF_4	23	23.36	0.36	3.999	0.430	10.761
		20.77	21.06	0.29	3.394	0.347	10.215

m_1 - samples weight before immersion $[g]$
m_2 - samples weight after immersion $[g]$
m_3 -oil mass in samples; $m_3 = m_2 - m_1[g]$

$$V_{pore} = V_{oil} = \frac{m_3}{\rho_{oil}}\left[cm^3\right];$$

$$\rho_{oil} = 0{,}8365\left[g/cm^3\right]$$

$$V_{samples} = h \cdot b \cdot l\left[cm^3\right]$$

[c]Porosity: $P = \frac{V_{pore}}{V_{samples}} \cdot 100\%$

Table 4. *Boride layers depth*

number of samples	activators	dept of boride layer [μm]								average value of boride layers depth[d] [μm]
		δ_1	δ_2	δ_3	δ_4	δ_5	δ_6	δ_7	δ_8	δ
I	4%NH_4FHF	68.5	62.5	95	87	83	78.5	74.5	89.5	79.813
		107	82	111	123.5	94.5	84	116	116	104.250
II	4%NH_4Cl	182.5	168.5	96.5	96.5	122.5	114.5	117.5	110.5	126.125
		119.5	119.5	121	129	138	111	106	139.5	122.938
III	4%NH_4Cl	129.5	98.5	85.5	99.5	136.5	117	117	148	116.438
		146.5	149.5	137	169.5	141	137.5	169.5	160.5	151.375
IV	1%NH_4FHF	136	97.5	130.5	127.5	116.5	148.5	134.5	148.5	129.938
	3%KBF_4	125	126	132	150	141.5	149	144	146.5	139.250
V	2%NH_4FHF	148	145.5	123	120.5	125.5	147	132	137	134.813
	2%KBF_4	76.5	147	116.5	110.5	90.5	146.5	149.5	197	129.250
VI	3%NH_4FHF	194	183	149.5	187	175	185	176.5	206.5	182.063
	1%KBF_4	149.5	126.5	146.5	171.5	124.5	200	175	198.5	161.500
VII	3%NH_4FHF	161.5	199	148	176	139.5	149.5	177	184.5	166.875
	1%NH_4Cl	120	127	117.5	194.5	167	165.5	111	170	146.563
VIII	2%NH_4FHF	120	120	161	177.5	177.5	162	159.5	132	151.188
	2%NH_4Cl	165	196.5	149.5	158.5	161.5	141	149.5	167	161.063
IX	1%NH_4FHF	106.5	126	76	112	129.5	123.5	91	99.5	108.000
	3%NH_4Cl	99.5	107	111	149.5	111.5	165	74.5	69	110.875
X	3%NH_4Cl	147	157	175.5	171	90	87.5	148.5	184.5	145.125
	1%KBF_4	106	82	149	144	134	129	121	123	123.500
XI	2%NH_4Cl	119	137.5	91	121	122	97.5	143.5	139.5	121.375
	2%KBF_4	149.5	126	126.5	140	136	149.5	124	157	138.563
XII	1%NH_4Cl	124	149.5	125	122	103.5	134.5	113.5	107	122.375
	3%KBF_4	111	129	112	115.5	120.5	115	130.5	129.5	120.375
XIII	1%NH_4FHF 2%NH_4Cl 1%KBF_4	98.5	136	149.5	132	132	139.5	133.5	129	131.250
		129.5	148.5	125	118.5	118.5	174	116.5	116.5	130.875
XIV	1%NH_4FHF 1%NH_4Cl 2%KBF_4	144	138	127	127.5	135	132	106.5	131.5	130.188
		129	107.5	120.5	105.5	121	144	144	144	126.938
XV	2%NH_4FHF 1%NH_4Cl 1%KBF_4	103.5	126	126	134	126.5	130.5	130.5	135	126.500
		129	106	141	126	126	139	136	130.5	129.188

[d] $\delta = \frac{\sum_{i=1}^{8} \delta_i}{8}\left[\mu m\right]$

Metallographic analyses were used to determine the quality of boride layers, so we examined the compactness and bond with the basic material, depth, cracks number, porosity, and percentage of FeB and Fe2B phase in boride layer. Samples were mechanically polished first at abrasive paper label 3 to 0000 (ASTM) and then by using felt soaked in alumina suspension, α-Al2O3 0.05 μm. After polishing had been completed, structure was etched with a 2% Nital solution. The dominant phase formed on the samples was found to be Fe2B phase. Depending on influence of activators, the depth of boride layers range was from 92 to 172 μm, leading to a diffusion controlled process.

3. THEORY/CALCULATION

Experiment planning of activators impact research on diffusion layer formation at boriding iron powder compacts was carried out. Simplex plan (Figure 1) with 15 experimental points was used (Krasovsky & Filaretov, 1982; Zedginidze, 1971). The results of simplex plan are presented in Table 5. The variation of the volume changes, porosity and the boride layers depth as a function of activators are presented in Figure 2.

Figure 1. *Experimental scheme (lattice Scheffe fourth – order)*

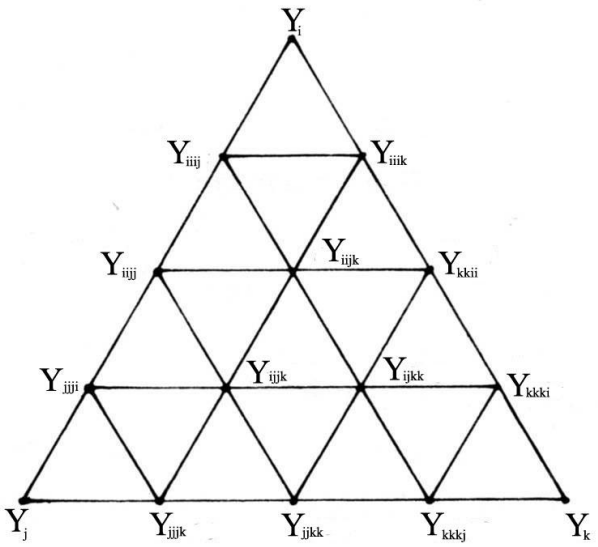

Table 5. *Plan of experiment and experimental results*

number of samples	plan of experiment						experimental results			
	contents of activators [%]			coded values of factors			volume changes [%]	porosity [%]	depth of boride layers [μm]	results
	NH_4FHF	NH_4Cl	KBF_4	X_1	X_2	X_3	ΔV_{av}	P_{av}	δ_{av}	Y
I	4	0	0	1	0	0	-0.099	16.430	131.062	Y_i
II	0	4	0	0	1	0	2.474	12.247	132.031	Y_j
III	0	0	4	0	0	1	-1.581	19.639	92.031	Y_k
IV	1	0	3	¼	0	¾	0.131	19.985	124.531	Y_{ikkk}

V	2	0	2	½	0	½	0.449	11.542	128.562	Y_{iikk}
VI	3	0	1	¾	0	¼	-0.985	18.106	129.969	Y_{iiik}
VII	3	1	0	¾	¼	0	1.949	6.378	171.781	Y_{iiij}
VIII	2	2	0	½	½	0	0.858	4.369	156.719	Y_{iijj}
IX	1	3	0	¼	¾	0	1.693	5.530	156.125	Y_{iiji}
X	0	3	1	0	¾	¼	4.449	8.888	134.312	Y_{jjjk}
XI	0	2	2	0	½	½	1.719	7.239	127.844	Y_{jjkk}
XII	0	1	3	0	¼	¾	0.427	7.977	121.375	Y_{jkkk}
XIII	1	2	1	¼	½	¼	0.676	8.240	134.594	Y_{ijjk}
XIV	1	1	2	¼	¼	½	2.449	7.246	133.875	Y_{ijkk}
XV	2	1	1	½	¼	¼	0.213	10.488	109.437	Y_{iijk}

Polynomial of fourth degree was used to obtained mathematical model for boriding process simulation. Polynomial is shown by relation (1):

$$y = b_i x_1 + b_j x_2 + b_k x_3 + b_{ij} x_1 x_2 + b_{ik} x_1 x_3 + b_{jk} x_2 x_3 + c_{ij} x_1 x_2 (x_1 - x_2) + c_{ik} x_1 x_3 (x_1 - x_3) + c_{jk} x_2 x_3 (x_2 - x_3) + d_{ij} x_1 x_2 (x_1 - x_2)^2 + d_{ik} x_1 x_3 (x_1 - x_3)^2 + d_{jk} x_2 x_3 (x_2 - x_3)^2 + b_{iijk} x_1^2 x_2 x_3 + b_{ijjk} x_1 x_2^2 x_3 + b_{ijkk} x_1 x_2 x_3^2 \quad (1)$$

where are activators used in experiment:

x_1 - NH_4FHF

x_2 -NH_4Cl

x_3 -KBF_4

and regression coefficients are:

$b_i; b_j; b_k; b_{ij}; b_{ik}; b_{jk}; c_{ij}; c_{ik}; c_{jk}; d_{ij}; d_{ik}; d_{jk}; b_{iijk}; b_{ijjk}; b_{ijkk}$; (i= 1, j= 2, k= 3)

It can be noted (Table 5.) that first three samples are related to influence of pure activators. From the 4th to 12th sample is presented influence of binary mixtures of activators in all combinations, samples 13, 14 and 15 give influences of ternary mixtures. After finishing of experiments, on the basis of obtained experimental results for volume changes, porosity and boriding layer depth (Table 5.) the unknown coefficients of polynomials are calculated by the following formulas:

$$b_i = y_i \quad (2)$$

$$b_j = y_j \quad (3)$$

$$b_k = y_k \quad (4)$$

$$b_{ij} = 4y_{iijj} - 2y_i - 2y_j \quad (5)$$

$$b_{ik} = 4y_{iikk} - 2y_i - 2y_k \quad (6)$$

$$b_{jk} = 4_{jjkk} - 2y_j - 2y_k \quad (7)$$

$$c_{ij} = 8/3(y_j - y_i + 2y_{iiij} - 2y_{ijjj}) \quad (8)$$

$$c_{ik} = 8/3(y_k - y_i + 2y_{iiik} - 2y_{ikkk}) \quad (9)$$

$$c_{jk} = 8/3(y_k - y_j + 2y_{jjjk} - 2y_{jkkk}) \quad (10)$$

$$d_{ij} = 8/3(4y_{iiij} + 4y_{ijjj} - 6y_{iijj} - y_i - y_j) \quad (11)$$

$$d_{ik} = 8/3(4y_{iiik} + 4y_{ikkk} - 6y_{iikk} - y_i - y_k) \quad (12)$$

$$d_{jk} = 8/3\left(4_{jjjk} + 4y_{jkkk} - 6y_{jjkk} - y_j - y_k\right) \quad (13)$$

$$b_{iijk} = 32\left(3y_{iijk} - y_{iijk} - y_{ijkk}\right) + 8/3\left(6y_i - y_j - y_k\right) - 16\left(y_{iijj} + y_{iikk}\right) - 16/3\left(5y_{iiij} + 5y_{iiik} - 3y_{ikkk} - 3y_{ijjj} - y_{jjjk} - y_{jkkk}\right) \quad (14)$$

$$b_{ijjk} = 32\left(3y_{ijjk} - y_{iijk} - y_{ijkk}\right) + 8/3\left(6y_j - y_i - y_k\right) - 16\left(y_{jjkk} + y_{iijj}\right) - 16/3\left(5y_{jjjk} + 5y_{ijjj} - 3y_{jkkk} - 3y_{iiij} - y_{ikkk} - y_{iiik}\right) \quad (15)$$

(16)

Where experimental results (Table 1) are: y_i, y_j, y_k, y_{iijj}, y_{ijjj}, y_{iijk}, y_{iiij}, y_{jjkk}, y_{ijjk}, y_{ijkk}, y_{iikk}, y_{iiik}, y_{ikkk}, y_{jjjk}, y_{jkkk} (i= 1, j= 2, k= 3)

Values of regression coefficients are given in Table 6.

Table 6. *Regression coefficients for polinomial of fourt deegre, equation (1).*

		Volume changes	Porosity	Depth
Regression coefficients	b_i	-0.099	16.430	131.062
	b_j	2.474	12.247	132.0.31
	b_k	-1.581	19.640	92.031
	b_{ij}	-1.317	-39.878	100.690
	b_{ik}	5.155	-25.970	68.062
	b_{jk}	5.092	-34.819	63.252
	c_{ij}	8.227	-6.632	86.083
	c_{ik}	-9.905	-1.461	-75.080
	c_{jk}	10.637	24.569	-37.669
	d_{ij}	18.773	-19.358	288.579
	d_{ik}	-11.815	125.453	62.760
	d_{jk}	22.115	-20.953	84.325
	b_{iijk}	-74.916	279.778	-3342.565
	b_{ijjk}	147.793	186.042	402.456
	b_{ijkk}	200.285	-216.647	1131.261

3.1 The validation of the model

Checking the adequacy of the mathematical model was carried out in two control points – K1 and K2 (Figures 2a, 2b, 2c). The validation of the model was checked by Student t – criteria.

$$t_{ki} = \frac{D_{ki}\sqrt{r}}{\sigma_y\sqrt{1+A_{ki}}} < t_{kr\,\alpha/k,f}, \quad (17)$$

Where is:

D_{ki} - maximum difference between calculated and actual properties values in investigated points, determined by equation:

$$D_{ki} = \bar{y} - \hat{y}_i \quad (18)$$

i= 1, 2, 3, ... n; and depends of control points number

$\bar{y}$ - value of the regression polynomial for all combinations of factor levels in selected control points

$\hat{y}_i$ - values obtained by experiment

r – number of repeated experiments in the plan points

σ_y – average square experiment error (experiment dispersion)

Deviation of standard results at measuring, used to determine experiment error, is calculated by dispersion analysis, equation (19).

$$\sigma^2 y = \frac{1}{n}\sum_i^n \left(y_i - \bar{y}_i \right)^2 \quad (19)$$

where are:

σ^2y - dispersion of experiment

y_i - values obtained by experiment

$\bar{y}_i$ - is mean values of experiment values sum

A_k – value which depends on the control points positions in the plan of experiment triangle which usually is determined for each plan (first, second, third, fourth degree) separately (Keddam & Chegroune, 2010; Krasovsky & Filaretov, 1982; Zedginidze, 1971).

For the fourth degree plan Ak is determined by equation:

$$A_{ki} = \left[\sum a_i^{\,2} + \sum a_{iijj}^{\,2} + \sum aiiij^2 + \sum a_{iilk}^{\,2}\right] \quad (20)$$

$$a_i = 1/3x_i\left(32x_i^{\,3} - 48x_i^{\,2} + 22x_i - 3\right); (a_1, a_2, a_3) = a_i \quad (21)$$

$$a_{iijj} = 4x_i x_j \left(1 + 16x_i x_j - 4x_i - 4x_j\right); (a_{1122}, a_{1133}, a_{2233}) = a_{iijj} \quad (22)$$

$$a_{iiij} = 16/3x_i x_j \left(8x_i^{\,2} - 6x_i + 1\right); (a_{1112}, a_{1222}, a_{2333}, a_{1113}) = a_{iiij} \quad (23)$$

$$a_{iijk} = 32x_i x_j x_k \left(3x_i - x_j - x_k\right); (a_{1123}, a_{1223}.a_{1233}) = a_{iijk} \quad (24)$$

α – level of probability (α = 0.01);

k_i – number of control points in which the validation of the model adequacy is executed *(i = 1, 2)*

f – number of freedom degrees for the results dispersion evaluation $\sigma^2{}_{\hat{y}}$

$$t_i \lessdot t_{kr} \quad (25)$$

If ti is less than tkr i.e. ti ‹ tkr, hypothesis of inadequacy is accepted. Model is then inadequate and vice versa.

Based on the Student t – criteria, the adequacy of the fourth level mathematical model was confirmed with 99% probability.

3.2Algoritham for a real solution determining

```
0010 REM PROGRAM FOR THE FOURTH DEGREE POLYNUM
0020 READ B1,B2,B3,B4,B5,B6,C1,C2,C3,D1,D2,D3,E1,E2,E3
0030 DATA 70.6,100.5,65.7,2,4,5,9,7,4,8,9,6,5,5,3
0031 DATA 514.53,737.2,51.73,-2209.23,743.29,2470.37
0040 INPUT R1,R2,R3,N,K
0050 INPUT E5

0060 FOR Y=R1 TO R2 STEP R3
0065 FOR X3=0 TO 1 STEP K
0100 H=1/N
0110 FOR I=1 TO N STEP 1
0120 Z1=(H)*(I-1)
0130 Z2=(H)*(I)
0140 GOSUB 200
0150 NEXT I
0155 NEXT X3
0156 NEXT Y
0160 END

0200 Z3=(Z1+Z2)/2
0210 X1=Z1
0220 GOSUB 500
0225 IF X2<0 THEN GO TO 240
0230 Y1=Y5
0240 X1=Z2
0250 GOSUB 500
0255 IF X2<0 THEN GO TO 270
0260 Y2=Y5
0270 X1=Z3
0280 GOSUB 500
0285 IF X2<0 THEN GO TO 440
0290 Y3=Y5
0300 Y4=ABS(Y3-Y)
0310 IF Y4>E5 THEN GO TO 340
0320 PRINT ″X1=″;X3,″X2=″;X2, ″X3=″;X3, ″Y=″;Y, ″YY=″;Y3
0330 GO TO 440

0340 B8=(Y1-Y)*(Y3-Y)
0350 B9=ABS (B8)
0360 IF B8=B9 THEN GO TO 390
0370 Z2=Z3
0380 GO TO 200
0390 B8=(Y2-Y)*(Y3-Y)
0400 B9= ABS (B8)
0410 IF B8=B9 THEN GO TO 440
0420 Z1=Z3
0430 GO TO 200
```

```
0440 RETURN

0500 X2=1-X1-X3
0510 A1=(B1)*(X1)+(B2)*(X2)+(B3)*(X3)+(B4)*(X1)*(X2)+(B5)*(X1)*(X3)
0520 A2=(B6)*(X2)*(X3)+(C2)*(X1)*(X2)*(X1-X2)+(C2)*(X1)*(X3)*(X1-X3)
0530 A3=(C3)*(X2)*(X3)* (X2-X3)+(D1)*(X1)*(X2)*(X1-X2)*(X1-X2)
0540 A4=(D2)*(X1)*(X3)* (X1-X3)*(X1-X3)+(D3)*(X2)*(X3)*(X2-X2)*(X2-X3)
0550 A5=(E1)*(X1)*(X1)* (X2)*(X3)+(E2)*(X1)*(X2)*(X2)*(X3)
0560 A6=(E3)*(X1)*(X2)* (X3)*(X3)
0570 Y5=A1+A2+A3+A4+A5+A6
0580 RETURN
```

Algorithm application for computer program requires entering following information:

- experiment plan
- experimental results for volume changes, porosity and depth boriding layers,
- regression coefficients
- borders to determine iso - lines
- step that depend on the lines density in the simplex triangle
- control points

4. RESULTS AND DISCUSSION

After the activation of program a dialog box appears that contains a table which is filled on the basis of the provided plan for the experiment and based on the obtained experimental results (volume changes, porosity and boroning layer depth). The program is designed to enable us to draw simplex triangle, (figures 2a, 2b and 2c), give us the value of regresion polynomial (1).

The value of regresional polynomial indicates obtained volume changes, porosity or boriding layer depth changes with the selected activator content (coordinates x1, x2 and x3), so these changes can be predicted in advance or specified. By analysis of iso lines, it can be seen where are obtained extreme values of observed changes. In Figure 2a, is shown pressed and boriding samples volume changes dependence of the mixture composition. Closed iso-line are obtained when a volume changing is 2.6% to -0.1%, which means that in these areas are achieved extreme values of boriding samples dimensional changes.

Maximum values, 2.7% and - 0.5%, in these areas were obtained by algorithm for computing. Such volume changes will be possible if boriding process is performed in mixtures which contain: 0.9% NH4FHF, 0.7% NH4Cl, 2.4% KBF4 and 1.7% NH4FHF, 1.7% NH4Cl, 0.6% KBF4, respectively. After boriding, due to the influence of boriding mixture and the presence of activated sintering, sample size may remain the same, or there may be shrinkage or increase in sample size.

a)

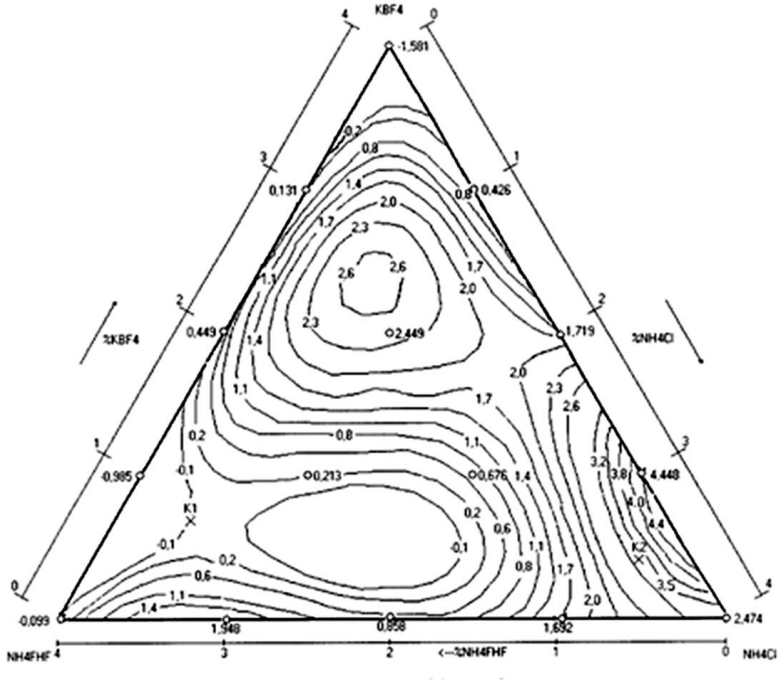
KBF4
NH4FHF
NH4Cl
%KBF4
%NH4Cl
<--%NH4FHF
K1
K2

b)

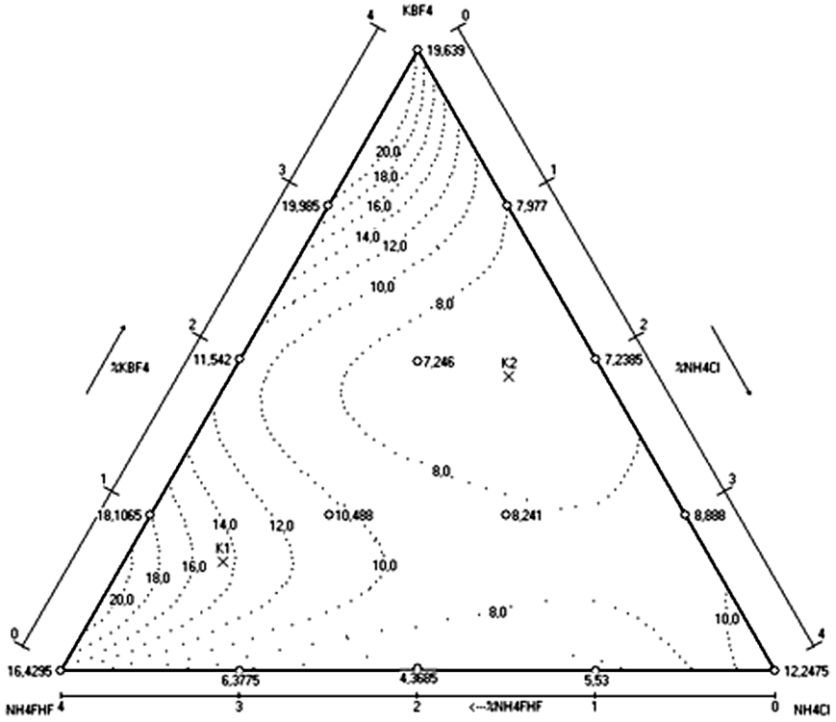
KBF4
NH4FHF
NH4Cl
%KBF4
%NH4Cl
<--%NH4FHF
K1
K2

c)

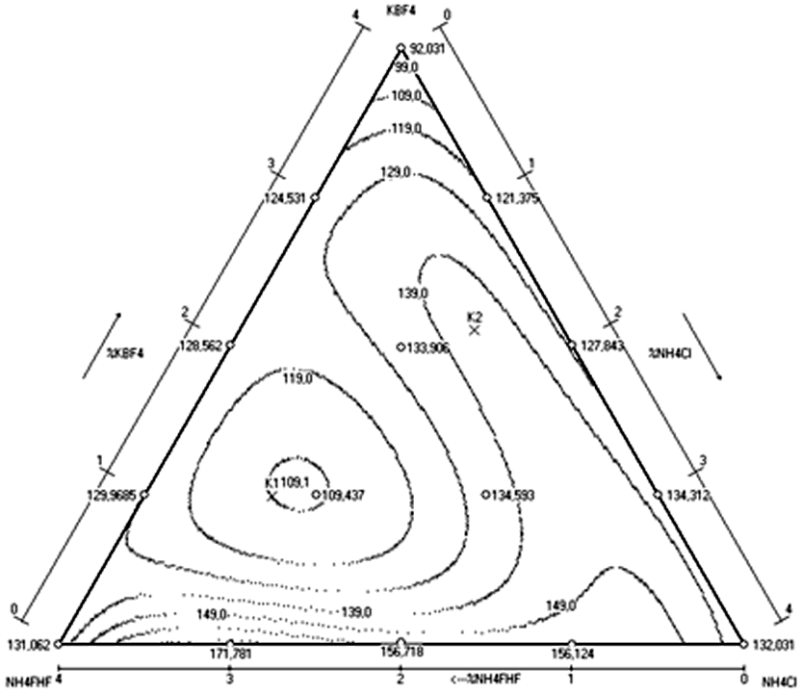

Figure 2. General principles followed by the pressed boroned samples observed changes from boriding composition mixture for a) volume changes b) porosity c) depth of boride layers of the pressed boroned samples (o - experimental points, • - points obtained by calculations, × - control points) (Celebi et al., 2005; Ivanov & Požega, 2008; Požega et al., 2009; Požega & Ivanov, 2008; Požega et al., 2009)

Influence of the mixtures composition for boriding on the volume changes for pressed and boriding iron powder samples is dual. In some samples was observed contraction, and in others increase in size, ie. expansion. Influence of boron - a saturation element, is dominated when volume is increased. As a result of boron atoms diffusion from boriding mixture to the surface layer of samples, there was an increase in sample size, thus and in volume.

By formation of diffusion layers on the pore surface volume increases, because the surface crossing of the pore channel reduces and a large number of pores disappears. Internal mass transport processes reduce the distance between particles of powder, resulting in the pressed samples shrinking. In samples where there is a shrinking, there is a reduction in porosity. This leads to reduction in pore volume and an increase in pressed samples density.

Application working by described algorithm allows us to pre-determine the volume change without practical experiment and allows optimization of the boriding process. Increased porosity of boriding samples, compared to the normal, is the consequence of insufficiently activated sintering. The quantity of activated sintering depends on diffusion coefficient, powder particle size and pressing pressure. During sintering the pores become orbiculate and at the final stage of sintering, open porosity transforms in closed porosity with isolated pores. By simulation of boriding process we can determine the activators percentage content and the adequate values of samples porosity, (figure 2b). The largest porosity of boriding samples, 19.985% are observed in the mixtures with 1% NH4Cl, 3% NH4FHF and 0% KBF4. On the other hand, the lowest porosity of 4.369% and most visible activated sintering was observed

on boriding samples in mixtures which containe 2% NH4Cl, 2% KBF4 and 0% NH4FHF, (table 3). In Figure 2c. is given the dependence of pressed samples and boriding samples depth changes from mixtures composition for boriding. It can be observed varying in depths of boriding layers due to the influence of different mixtures composition and the uneven effects of activator. The depth of diffusion layer depends on the active and adsorbed boron atoms concentration on the surface of the sample. Boron saturation in the gas environment in the presence of a large number of pores, allowed obtaining of boriding layers higher depth. Concentration of diffunded element (boron) is increased at a significantly greater depth, since the saturation proceeded from the sample surface, and also from pore surface. At boriding layer depth of 109.1 μm was obtained a closed iso-lines, which means that in this area reached depth of boriding layers are extreme. Experimentally obtained value in this area amounts to 109. 437 μm. Such depth would be obtained if the boriding performed in mixtures containing 2% NH4FHF, 1% NH4Cl, 1% and 1% KBF4.

CONCLUSION

Analysis and evaluation of the basic indicators for the quality boride layers obtain was done by computer program during the emergency measures caused by the COVID-19 pandemic adopted by the Government of the Republic of Serbia and work from home. The presented paper is the achievement of efficient science performance of our research group for the given measures during the covid-19 pandemic.

Algorithm for computer program proposed in this work is a simple and convenient tool for simulation of volume changes, changes in porosity and depth boriding layer as a function of activators.

By adjusting basic mixture which is modified by the addition of activators, it makes it possible to optimize the properties of borides layers. By algorithm it is able to predict the most suitable activator composition. In this way can be reduced number of practical experiments, new product development time and work of researchers during the COVID-19 pandemic. The obtained results are part of broader continued and ongoing investigations of new substances that have a positive impact on the boriding metallic materials produced using powder metallurgy in the frame of our research group (Krasovsky & Filaretov, 1982; Ivanov & Požega, 2008; Požega et al., 2009; Požega & Ivanov, 2008; Požega et al., 2009; Miletić & Stanojević, 2018; Miletić et al., 2016).

ACKNOWLEDGMENTS

The authors are grateful for the assistance in computer program preparation to his colleague Ćerim Abazi.

The research presented in this paper was done with the financial support of the Ministry of Education, Science and Technological Development of the Republic of Serbia, within the financing of scientific research work in the Institute of Mining and Metallurgy Bor, according to the Contract No. 451-03-9/2021-14/200052, and at the University of Belgrade, Technical Faculty in Bor, according to the Contract No. 451-03-9/2021-14/200131.

REFERENCES

Allaoui, O., Bouaoudja, N., & Saindernan, G. (2006). Characterization of boronized layers on a XC38 steel. *Surface and Coatings Technology*, 201(6), 3475-3482.

Berger, A., Grigoriev, A., & Winokurow, A. (2017). An efficient algorithm for the single facility location problem with polyhedral norms and disk-shaped demand regions. *Computational Optimization and Applications*, 68, 661-669.

Campos, I., Baustina, O., Ramirez, G., Islas, M., De la Parra, J., Zúñiga, L., (2005).The matrix which is not affected by boron. *Applied Surface Science*, 243, 429-436.

Celebi, G., Ipek, M., Bindal, C., Ucisik, H. (2005). Some mechanical properties of borides formed on AlSi 8620 steel. *Materials Forum*, 39, 456-460.

Chatterjee, F. (1989). *Surface Modification Technologies*. T S Sundarshan, USA, Marcel Dekker Inc

Dong, X., Hu, J., Huang, Z., Wang, H., Gao, R., Guo, Z. (2009). Microstructure and properties of boronizing layer of Fe-based powder metallurgy compacts prepared by boronizing and sintering simultaneously. *Science of Sintering*, 41, 199-207.

Erdemir, A., & Bindal, C. (1995). Formation and self-lubricating mechanisms of boric acid on borided steel surfaces. *Surface and Coatings Technology*, 76-77, 443-449.

Genel, K., Ozbek, I., Kurt, A., Bindal, C. (2002). Boriding response of AISI W1 steel and use of artificial neural network for prediction of borided layer properties. *Surface and Coatings Technology*, 160, 38-43.

Hunger, H., & Trute, G. (1994). Boronizing to produce wear-resistant surface layers. *Heat Treatment of Metals*, 2,31-39.

İpek, R., Selçuk, B., Karamiş, M., Kuzucu, V., Yücel A. (2000). An evaluation of the possibilities of using borided GG25 cast iron instead of chilled GG25 cast iron (surface properties). *Journal of Materials Processing Technology*, 105, 73-79.

Ivanov, S., & Požega, E. (2008). Influence of the composition of the boroning mixture on the dimension change of pressed and boroned samples from iron powder. *Science of Sintering*, 40, 197-205.

Jain, V., & Sundararajan, G. (2010). Influence of the pack thickness of the boronizing mixture on the boriding of steel. *Surface and Coatings Technology*, 149, 21-26.

Kayacan, Ö., Şahin, S., Taştan, F. (2010). A study for boronizing process within nonextensive thermostatistics. *Mathematical and Coputational Applications*, 15, 14-24.

Keddam, M., & Chegroune, R. (2010). A model for studying the kinetics of the formation of Fe_2Be boride layers at the surface of a gray cast iron. *Applied Surface Science*, 256, 5025-5030.

Keddam, M. (2004). A kinetic model for the borided layers by the paste-boriding process. *Applied Surface Science*, 236, 451-455.

Keddam, M., & Chentouf, S. (2005). A diffusion model for describing the bilayer growth (FeB/Fe_2B) during the iron powder-pack boriding. *Applied Surface Science*, 252, 393-399.

Krasovsky, I., Filaretov, F. (1982). *Plans of Experiment*. Minsk, Publishing house of BSU-Belarusian State University (in Russian)

Makuch, N. (2020). Nanomechanical properties and fracture toughness of hard ceramic layer produced by gas boriding of inconel 600 alloy. *Transactions of Nonferrous Metals Society of China*, 30(2), 428-448.

Makuchp, N., Dyiarski, P., Kulka M., Piasecki, A., Tuli'nski, M., Majchrowski R. (2019). Influence of niobium and molybdenum addition on microstructure and wear behavior of

laser-borided layers produced on Nimonic 80A-alloy. *Transactions of Nonferrous Metals Society of China*, 29(2), 322-337.

Meric, C., Sahin, S., Backir, B., Sinan Koksal, N. (2006). Investigation of the boronizing effect on the abrasive wear behavior in cast iron. *Materials and Design*, 27, 751-757.

Miletć, S., Stanojević Šimšić, Z., (2018). Strategic analysis of organization by AHP method, Innovation as an initiator of the development "innovations – basis for development" International Thematic Monograph – Thematic Proceedings, University Business Academy in Novi Sad, Faculty of Applied Management, Economy and Finance, Belgrade, MEFkon 2018, December 6th Belgrade, 289-307.

Miletić, S., Bogdanović, D., Milanović, D., (2016). Advantages of implementation the process model for sustainable business operations of mining companies. *Journal Mining and Metallurgy Institute Bor*, 3, 71-82.

Novik, S. (1971). *Mathematical methods for planning experiments in metal science.* Moscow, Moscow Institute of Steel and Alloys. (in Russian)

Nyborg, L., Nylund, A., Olefjord, I. (1987). *Thickness determination of oxide layers on spherical shaped metal powders by ESCA*. Proc. of ESCASA 1987. Stuttgart

Ozdemir, O., Usta, M., Bindal, C, Ucisik, H. (2006). Hard iron boride (Fe_2B) on 99.97 wt% pure iron. *Vacuum*, 80, 1391-1395.

Özge, B., Duygu, A., Lütfi, M., Duman, Ï. (2016). Synthesis of niobium borides by powder metallurgy methods using Nb_2O_5, B_2O_3 and Mg blends. *Transactions of Nonferrous Metals Society of China*, 26(3), 747-758.

Paul, SK, Chowdhury, P. (2020). A production recovery plan in manufacturing supply chains for a high-demand item during COVID-19. *Int J Phys Distrib Logist Manag* 1-22. https://doi.org/ 10.1108/IJPDLM-04-2020-0127.

Požega, D. E. (2008). *Activators influence on the diffusion layer formation at boronizing of pressed iron powd*er. [Master's Thesis] Serbia, SRB; University in Belgrade, Technical faculty in Bor.

Požega, E., Ivanov, S. (2008). Influence of activators on constitutes of diffusion layer at boronizing pressed samples from iron powder. *Hemijska Industrija*, 63,164-169. (in Serbian)

Požega, E., Ivanov, S., Abazi, Ć. (2008). Computer programme for polynomial of fourth degree. *Inovacije i razvoj*, 2, 51- 62. (in Serbian)

Požega, E., Ivanov, S., Conić, V., Čađenović, B. (2009). The possibility of the boronizing proces on the pressed samples of iron powder. *Hemijska Industrija*, 63, 253-258. (in Serbian)

Požega, E., Ivanov, S., Ivanović, A. (2009). Influence different chemical composition and percente rate of added activators on depth of boride layer. *Zaštita Materijala*, 50, 99-104. (in Serbian)

Ramirez, G., Campos, I., Balankin, A. (2007). Fracture toughness of iron boride layers obtained by paste boriding process. *Materials Science Forum*, 553, 21-26.

Segal, S., Gerstel, D. (2020). The Global Economic Impacts of COVID-19. https://www.csis.org/analysis/global-economicimpacts-covid-19.

Selçuk, B., İpek, R., Karamiş, B., Kuzucu, V. (2000). An investigation on surface properties of treated low carbon and alloyed steels (boriding and carburizing). *Journal of Materials Processing Technology*, 103, 310-317.

Sen, S., Sen, U., Bindal, C. (2005). An approach to kinetic study of borided steels. *Surface and Coatings Technology*, 191, 274-285.

Sinha, K. (1991). *Heat treating*. ASM Handbook. Ohio, USA, ASM International, Materials Park

Stojanović, Ž., Stanisavljev, S. (2013). Protection of parts of mechanical systems by multicomponent boronizing methods. *Zaštita materijala,* 54(4), 381-388. (in Serbian)

Stojanović, Ž., Stanisavljev, S., Erić, S., Đurđić, M. (2017). Increasing the efficiency of forging tools by thermal diffusion boronizing. *Zaštita materijala,* 58(1), 22-29. (in Serbian)

Voroshnin, G., Lyakhovich, S., Lovshenko, G., Protasevich, F. (1977). Chemical heat treatment of cerment materials Minsk, Science and Technology. (in Russian)

Xu, H., Xi, K., Gao, W. (1997). Improving the mechanical properties of boronized lazers by superplastic boronizing. Journal of Materials Processing Technology, 65, 94-98.

Zedginidze, G. (1971). Mathematical design of an experiment for the study and optimization of the mixtures properties. Tbilisi, Metsniereba. (in Russian)